3.4 OBSERVATIONS OF TWO POSITIVE CLOUD-TO-GROUND STORMS OBSERVED DURING STEPS

Sarah A. Tessendorf* and Steven A. Rutledge
Colorado State University, Fort Collins, CO

1. INTRODUCTION

The Severe Thunderstorm Electrification and Precipitation Study (STEPS; Lang et al. 2004) field campaign took place between 17 May and 20 July 2000 in eastern Colorado and western Kansas. STEPS research aims to identify relationships between dynamics, microphysics, and electrification in storms on the High Plains, where a high percentage of storms that produce anomalous positive cloud-to-ground (CG) lightning have been documented (Carey et al. 2003). This study presents radar and lightning observations of two positive CG-producing storms observed during STEPS.

On 29 June 2000, a positive CG-producing severe thunderstorm propagated through the STEPS multiple-Doppler radar network between 2130 UTC[1] (29 June) and 0115 (30 June) producing large hail and an F1 tornado, in addition to copious lightning. This storm has received much attention by the STEPS community (MacGorman et al. 2005, Tessendorf et al. 2005, Wiens et al. 2005).

By 2356 on 22 June 2000, a cell at the southern end of an extensive MCS developed in the western lobe of the STEPS radar network. Another cell just north of CHILL merged with this first cell just after 0000 (23 June). Between 0000-0030 surface reports indicated that this storm produced hail up to 1 inch and surface winds near 30 m s^{-1}. By 0300, this storm system had exited the eastern lobe of the radar network, but persisted on the southern end of a well-organized MCS.

2. DATA AND METHODS

Instrumentation and observing systems operated during STEPS that are most central to this study included three S-Band Doppler radars (two of which were polarimetric research radars) for mapping the three-dimensional structure of precipitation and storm winds, the National Lightning Detection Network (NLDN; Cummins et al. 1998), and the 3-D Lightning Mapping Array (LMA; Rison et al. 1999) operated by New Mexico Institute of Mining and Technology.

2.1 Radar data processing

The CSU-CHILL polarimetric Doppler radar, the National Center for Atmospheric Research (NCAR) S-Pol polarimetric Doppler radar, and the Goodland, Kansas National Weather Service (NWS) WSR-88D radar (KGLD) comprised the triple-Doppler radar network used to take the radar measurements. The three radars were arranged in a rough equilateral triangle configuration with approximately 60-km sides (Fig. 1).

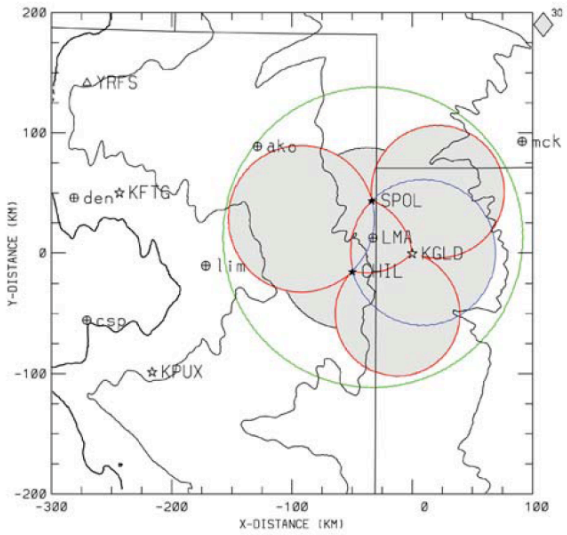

Figure 1. Nominal areas of coverage (shading) by the triple-Doppler radar network (from Lang et al. 2004).

The dual linear polarization capability, on the CSU-CHILL and NCAR S-Pol radars, enables these radars to detect hydrometeor shape and size that, when combined with air temperature, can be used to infer the dominant hydrometeor type for a given resolution volume.

* *Corresponding author address*: Sarah A. Tessendorf, Colorado State Univ., Dept. of Atmospheric Science, Fort Collins, CO 80523-1371; e-mail: saraht@atmos.colostate.edu

[1] All times hereafter are listed in UTC.

Wind field syntheses were completed for 11 volume scans during the period 2356 (22 June)-0108 (23 June) and 37 volume scans during the period 2130 (29 June)-0115 (30 June). The radar data were interpolated onto a Cartesian grid using NCAR's Sorted Position Radar INTerpolator (SPRINT). Grid resolution was 0.5 km in both the horizontal and vertical directions. After the grid interpolation, the velocity data were globally unfolded by means of NCAR's Custom Editing and Display of Reduced Information in Cartesian Space (CEDRIC) software (Mohr et al. 1986). The three dimensional wind fields were computed using the radial velocities from the CSU-CHILL and KGLD radars. The speed and direction of storm movement were calculated and used for the advection parameters. The vertical velocities were obtained using a variational integration of the continuity equation (O'Brien 1970).

The polarimetric data were edited to eliminate noise, clutter, and suspect data following the methods outlined in Ryzhkov and Zrnic (1998). The processed data were then gridded in the same manner as described above. A fuzzy-logic hydrometeor classification scheme, (hereafter FHC), adapted from Liu and Chandrasekar (2000) and Straka et al. (2000), was implemented for the Cartesian gridded data to estimate bulk hydrometeor types within the storm (Tessendorf et al. 2005). Hydrometeor echo volumes were also calculated for each radar scan time by multiplying the number of grid points (N) that satisfied the FHC category of interest by the volume of a grid box (0.125 km^3). Time series of the polarimetric results and the vertical motion estimates were then compared.

2.2 Lightning data processing

The New Mexico Tech LMA measures the time and three-dimensional location of very high frequency (VHF) radiation sources emitted by lightning discharges. For a given lightning flash, the LMA may locate hundreds to thousands of such sources resulting in detailed maps of the total lightning activity. To interpret these data, we use the bi-directional discharge model (Kasemir 1960, Mazur and Ruhnke 1993) which assumes that flashes initiate in regions bordered by horizontal charge layers of opposite sign (i.e. regions of strong electric field), and then propagate bi-directionally into the two charge layers. Keeping in mind that the negative breakdown component of a lightning flash is noisier at VHF, which makes it more frequently detected by the LMA than the positive breakdown component, we can infer the location and sign of charge regions based on the location of flash initiation, and the temporal evolution and relative number of LMA sources on either side of the flash initiation location. Furthermore, we also assume that negative breakdown passes through regions of net positive charge, and vice versa. For example, if the LMA sources from a flash initially propagated upward and there were relatively fewer sources below the initiation height than above it, we infer that the flash initiated above a negative charge layer and below a layer of positive charge. To determine total (CG plus IC) flash rates from the LMA data, we used an algorithm developed at New Mexico Tech (Thomas et al. 2003) that sorts the LMA sources into discrete flashes.

3. OBSERVATIONS

3.1 Overview

A trough line had set up in eastern Colorado by 1400 on 22 June 2000. Around 1900 a line of convection was observed on radar situated along the trough line and extending from northeastern Colorado in to the panhandle of Nebraska. A surface wind shift line was evident in the 2100 surface observations, in conjunction with the trough line, with southerly winds east of the line and northerly winds to the west of it. Surface temperatures in the STEPS domain were near 90 °F, with surface dew point temperatures near 50 °F (not shown). CAPE values were marginal, around 500 J kg^{-1} based on MGLASS soundings taken in the area (Fig. 2).

Near 2330, a cell on the southern end of the line of convection entered the western portion of the STEPS radar network. This cell dissipated by 0000, but a new cell directly to its southeast developed by 2356 (Fig. 3; hereafter Cell A). There were only two CG flashes observed in cell A[2], both of positive polarity. Another convective cell was also observed at this time just north of the CSU-CHILL radar, propagating to the northeast (hereafter Cell B). A few positive and negative CG

[2] Even though Fig. 3 shows some negative CG strikes in the early path of cell A (around x= -80, y= 30), those CGs were from convection not discussed in this study that developed in the initial location of Cell A after it had moved to the northeast and merged with Cell B.

strikes were observed with Cell B. These two cells merged by 0009 (hereafter Cell AB). Near the time of the merger, a new cell (hereafter Cell C) developed to the south of Cell AB. Beyond that time, Cells AB and C continued to propagate to the east-northeast and evolved into a linear convective system (hereafter Line ABC) near 0108. During the merger process of Cells A and B, the storm only produced negative CGs on its far eastern flank, but about 10 minutes after their merger, a peak positive CG flash rate of near 10 flashes per minute was observed. Just after the peak in positive CG flash rate, the peak total flash rate was observed near 500 per minute. Beyond 0030, the storm remained a predominantly positive CG-producer until dissipation. Another group of cells developed to the southeast of Line ABC as it was dissipating near 0150. These new cells formed a linear convective system that propagated northeastward out of the STEPS radar network. This paper will focus on Cells A, B, AB, and C.

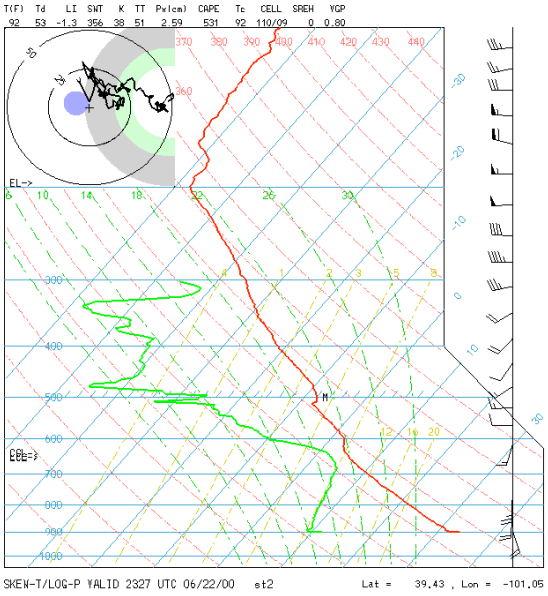

Figure 2. MGLASS sounding at 2327 UTC from near Goodland, Kansas.

3.2 Time series

At the beginning of the analysis period, the maximum updraft was already 30 m s^{-1} in both Cells A and B (Fig. 4). By 0010 when Cells A and B were beginning to merge, the maximum updraft quickly increased to 45 m s^{-1} near the apex of the merger, where it remained for almost an hour. By the end of the analysis period, the maximum updraft was observed near 50 m s^{-1} in Cell C, while it had weakened to near 30 m s^{-1} in Cell AB. The graupel echo volume (hereafter graupel EV) maximum was centered around 6 km MSL[3] until 0050, when its maximum deepened to between 5-9 km (Fig. 4). At this time, when graupel EV was at its maximum in the analysis period, the updraft was also at its maximum speed. Graupel EV reached heights up to 16 km at times, indicating this was obviously a very deep convective storm. The hail echo volume (hereafter hail EV) maximum was centered around 8-9 km and peaked between 0010-0050 (Fig. 4).

Graupel was already detected by the FHC algorithm at the beginning of the analysis period (Fig. 5). As mentioned above, graupel EV peaked at the end of the analysis period. However, the graupel EV peak was not coincident with the peak in updraft volume greater than 10 m s^{-1} (hereafter UV10), which peaked near 0025 (Fig. 5). The peak in UV10 was coincident with the peak in CG flash rate (mostly positive CGs) and hail EV. UV10 decreased after 0025 until the end of the analysis period. What appears to have happened is that as Cell AB began to dissipate and lose UV10, the hail fell out. However, during this same time, the maximum updraft in Cell C was very high, but its volume was lower relative to Cell AB. Thus, the total hail EV seems to relate more to UV10 than maximum updraft.

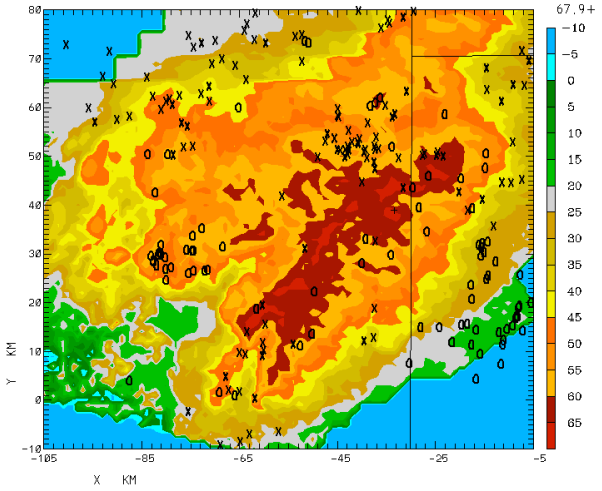

Figure 3. Swath of composite reflectivity from the CSU-CHILL radar accumulated for the period 2356-0108 on 22 June 2000. NLDN cloud-to-ground lightning strikes are overlaid with a black 'O' for negative strikes and a black 'X' for positive strikes. The '+' symbol represents the location of maximum reflectivity (67.9 dBZ) for the entire swath.

[3] All heights hereafter are in Mean Sea Level (MSL).

The total lightning flash rate (hereafter LFR) was already near 150 per minute at the beginning of the analysis period, and rapidly increased to around 400 per minute by 0010, coincident with the beginning of the cell merger process (Fig. 5). The LFR peak, which occurred just after 0030, was very impressive at approximately 500 per minute. LFR had a very similar trend as graupel EV (Fig. 5), which would be expected since ice-ice collisions have been shown to be important in charging processes (Takahashi 1978). The lower temporal resolution of the radar data to that of the lightning (LMA) data likely contributes to the smoother appearance of the graupel EV curve.

The positive CG flash rate was typically 1-3 per minute, except during its peak at 0025 (just after cells A and B merged) when it reached 10 per minute (Fig. 5). Between 0011-0022, during the cell merger, the positive CG flash rate was zero, and only negative CG flashes were observed. The negative CG flash rate during this time was at its peak of 3-4 per minute (Fig. 5). The negative CG flash rate was typically 1-2 per minute before and after this time period (Fig. 5). More details on the charge structure and location of the negative CGs between 0011-0022 and the positive CGs in the positive CG flash rate peak near 0025 will be discussed in following section.

3.3 Charge structure

In Figure 6, a maximum of LMA sources around 9 km is evident from the beginning of the analysis period. This generally corresponded to a relatively well-defined and persistent inferred positive charge layer at this height during this time period (not shown). After 0010, near the time of the cell merger, this maximum in LMA sources deepened and was more centered around 8 km (Fig. 6). Flash rates at this point exceeded 400 per minute. The maximum of LMA sources corresponds to a temperature of approximately −20 °C.

As might be expected from the extraordinary flash rates, the charge structure of this storm system was very complex, and discrete charge layers representative of the entire storm at any given time could not realistically be deciphered. However, we will attempt to describe the general charge structure that was seen in the LMA data until 0030 (the temporal extent of our detailed LMA analysis at this point), especially during periods of interesting CG activity. It is easier to do this if we individually discuss the charge structure of individual regions of the storm, in particular the eastern flank (i.e. anvil region), the northern and central portions (formerly Cell A and Cell B, respectively), and the southern portion (Cell C).

The eastern flank of storm (i.e. the anvil area and reflectivity overhang) consistently exhibited an area of inferred positive charge between 7-10 km, with inferred negative charge above that at 10-12 km (Fig. 7c). The negative CGs associated with this storm, especially in the period between 0011-0022 when negative CG lightning dominated, were primarily located in the far eastern flank of the storm, under this inverted dipole. The CG flashes typically originated from 9-10 km, tapping the upper negative charge. Reflectivity in the anvil area was fairly low (less than 20 dBZ; Fig. 7c), and unfortunately the scan sector from CSU-CHILL did not include this portion of the storm to identify hydrometeors via polarimetric radar observations (specifically vertically oriented ice would have been of particular interest). However, the core of the storm was mostly graupel echo with some small and large hail (Fig. 7b,d). Figure 7a also shows the time when Cells A and B had just merged, and when Cell C was detected south of the Cell AB merger (near x = -55, y = 10).

The northern portion of the analysis area (i.e. the area that was formerly Cell A) had multiple charge layers, and little to no CG activity until 0024 (there were only two positive CG flashes near 0002). A generalization of this charge structure from 2350-0020 could be termed a double dipole or a normal tripole with an upper screening layer, where inferred negative charge was present above 10 km, inferred positive charge resided between 8-10 km, another layer of inferred negative charge was observed between 6-8 km, and a second layer of positive charge resided between 4-6 km (not shown). Four-layer charge structures have also been documented by Stolzenburg et al. (1998) in convective updraft regions. The observed charge four-layer charge structure in Cell A was mostly in regions of updraft. By 0010 (the beginning of the merger with Cell B), the charge layers in this portion of the storm became very complex and difficult to generalize. However, positive charge was observed over a great depth of the storm (between 4-10 km). By 0024, this portion of the storm was producing abundant positive CG lightning (Fig. 8). These positive CGs typically originated around 7

km and typically came to ground below a region of inferred lower negative charge[4].

Figure 8 illustrates the radar structure during the time of peak positive CG lightning production. In Fig. 8a, it is apparent that the storm is elongated with a north-south orientation, the northern portion formerly Cell A, and the central portion formerly Cell B, with Cell C at the southernmost tip. The updraft is on the eastern (leading) flank and the positive CG lightning activity is clustered in the northernmost region of this storm. A large fraction of the upper levels of the storm contain precipitation ice in the forms of graupel and hail EV (Fig. 8b). An overhang in reflectivity is evident, surrounding the main updraft (greater than 25 m s^{-1}), in Fig. 8c. In a vertical projection, it is evident that the cluster of positive CG strikes comes to ground below the main core of the storm, where lower negative charge was observed and hail was detected to be falling out of the storm (Fig. 8c,d).

The central portion of the analysis area (and formerly Cell B) had a general inverted charge structure (see Fig. 7c). Upper negative charge was inferred between 9-12 km, with a region of main positive charge between 6-9 km, and lower negative charge from 4-6 km (the lower negative charge is not evident in the flashes shown in Fig. 7). Few CGs were observed within this portion of the storm, but those that were observed (in the first 20 minutes of the analysis period) were of positive polarity. By 0015, shortly after Cell B merged into Cell A, the charge layers were much more complex. Nonetheless, as in the former region of Cell A, there seemed to be a much deeper positive charge region at this point (from 5-10 km).

Cell C exhibited a fairly persistent inverted tripole charge structure. Upper negative charge was inferred between 10-12 km, main positive charge between 6-10 km, and lower negative charge between 4-6 km (not shown). The charge structure of Cell C and the eastern flank/anvil of this storm system exhibited much more straightforward and persistent charge layers. Even Cells A and B exhibited relatively simple charge layers prior to their merger. It was evident that the charge layers in Cells A and B became more complex after they merged into Cell AB, and a much deeper layer of positive charge was observed.

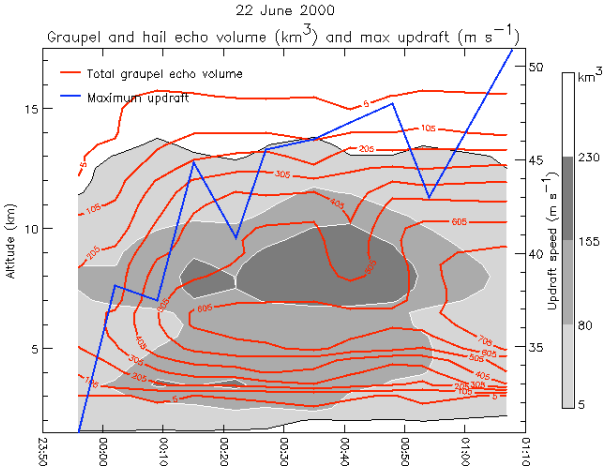

Figure 4. Time-height contours of total graupel echo volume (red contours) and total hail echo volume (gray shaded contours), and maximum updraft time series (values on right axis) for 22 June 2000. The statistics calculated in this time series include the volumes of both Cells A and B at 2356 and 0002, and of Cells AB and C for 0009-0108.

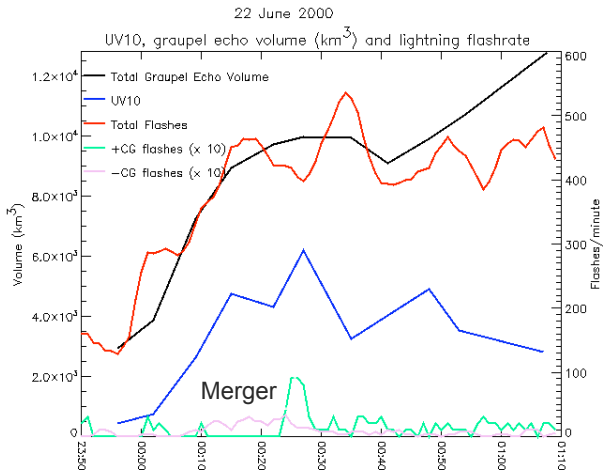

Figure 5. Time series of updraft volume greater than 10 m s^{-1} and graupel echo volume (left axis), total lightning flash rate from the LMA data (right axis), and the positive and negative CG flash rates (multiplied by 10 to fit on right axis) for 22 June 2000. The statistics include the same storm cell volumes as in Fig. 4.

[4] Recall from section 2.2 that positive breakdown is less noisy at LMA frequencies and therefore is not detected as well with the LMA. In addition, with the high flash rates observed in this storm system, it was difficult to assess the initiation height and charge layers associated with each positive CG flash. Negative breakdown associated with negative CG flashes was detected much better with the LMA and thus we are much more confident with our estimates of flash initiation height and associated charge layers in those cases.

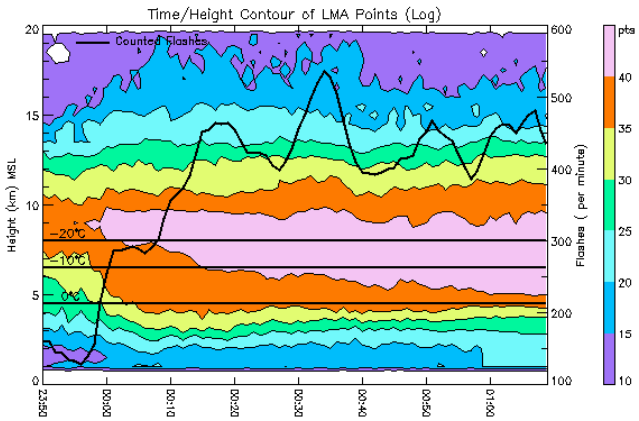

Figure 6. Time-height contours of the total number of LMA sources (color-shaded in logarithmic units) with the total flash rate time series overlaid in black for 22 June 2000.

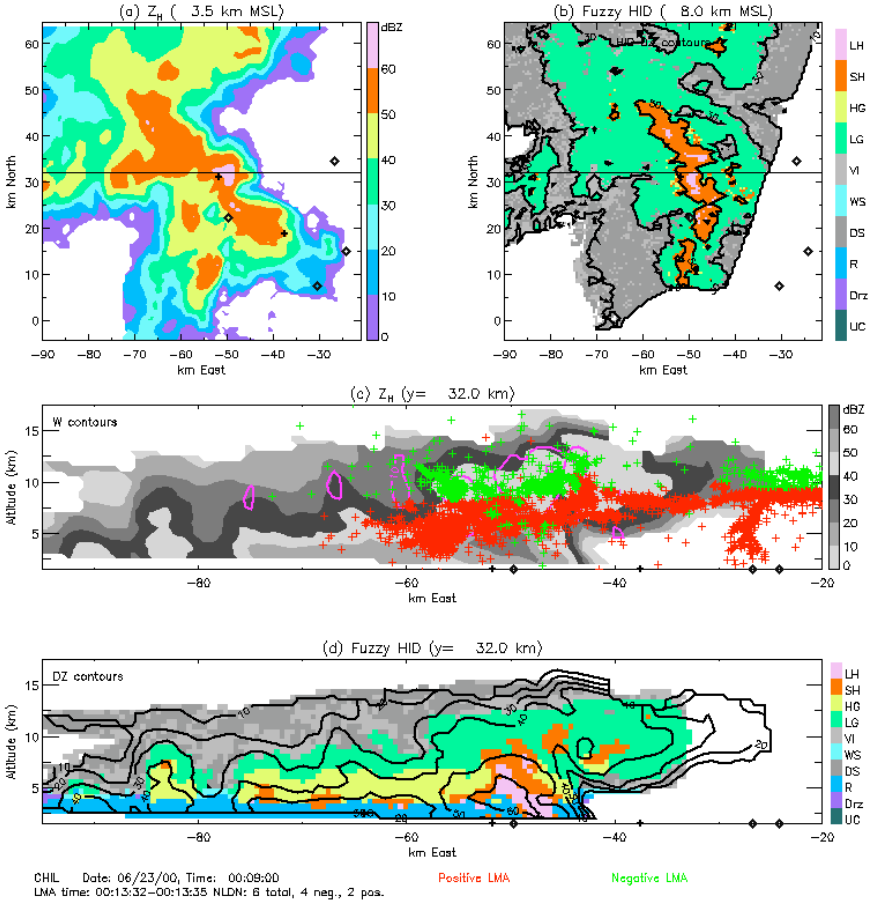

Figure 7. KGLD, CSU-CHILL, and LMA data at 0009 on 23 June 2000: a) KGLD reflectivity at 3.5 km; b) FHC (from CSU-CHILL) at 8 km with a black CSU-CHILL reflectivity contours every 20 dBZ, beginning with 10 dBZ; c) grayscale KGLD reflectivity at y = 32 km with updraft contours every 10 m s^{-1}, beginning with 10 m s^{-1}, overlaid in pink; and d) FHC (from CSU-CHILL) at y = 32 km with KGLD reflectivity contours every 10 dBZ, beginning with 10 dBZ, overlaid in black for reference. LMA sources from approximately 7 flashes (including one negative CG) between 00:13:32-00:13:35 as positive (red) and negative (green) charge are overlaid in (c). NLDN strikes between 0009-0015 are overlaid in all panels, with a black 'x' for positive and black diamond for negative CG flashes.

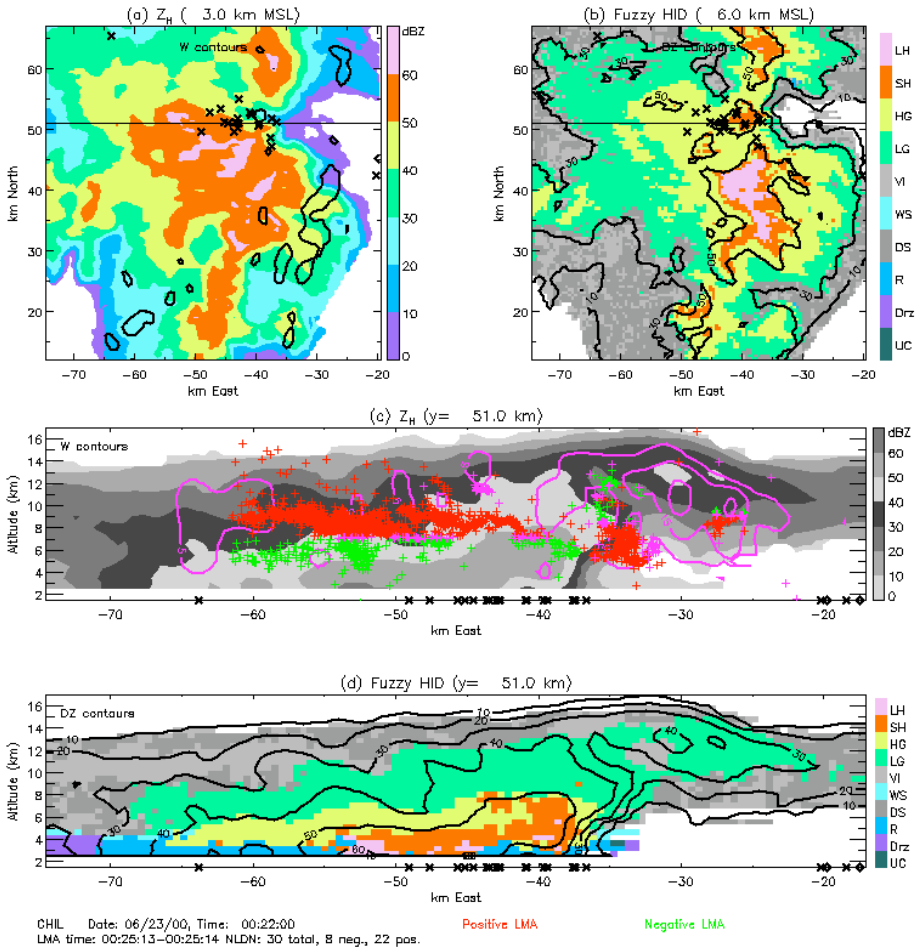

Figure 8. CSU-CHILL and LMA data at 0022 on 23 June 2000: a) CSU-CHILL reflectivity at 3 km with updraft contours at 5 m s^{-1} overlaid in black; b) FHC at 6 km with reflectivity contours every 20 dBZ, beginning with 10 dBZ, overlaid in black; c) grayscale CSU-CHILL reflectivity at y = 51 km with updraft contours every 10 m s^{-1}, beginning with 5 m s^{-1}, overlaid in pink; and d) FHC at y = 51 km with reflectivity contours every 10 dBZ, beginning with 10 dBZ, overlaid in black. LMA sources from approximately 6 flashes (including one positive CG) between 00:25:13-00:25:14 as positive (red) and negative (green) charge are overlaid in (c). NLDN strikes between 0022-0025 are overlaid in all panels, with a black 'x' for positive and black diamond for negative CG flashes.

4. COMPARISON WITH 29 JUNE 2000

The environment on 29 June was conducive for strong, isolated convection with CAPE values of 1254 J kg^{-1} and substantial shear (not shown). CAPE was only measured at a marginal value of 500 J kg^{-1} on 22 June (see Fig. 2). Nonetheless, the convection on 22 June was as strong as that on 29 June, at least as revealed by the dual-Doppler analyses. Maximum updrafts in 29 June were as high as 50 m s^{-1}, which is the same as in 22 June (Figs. 4, 9). However, the storm on 29 June was a well-organized supercell, while the convection on 22 June was much more multicellular and continually evolved into linear convective systems. Both storms were vertically developed, with graupel EV in both reaching heights of 15 km (Figs. 4, 9). Hail EV was also present through a great depth (cloud base to 13 km) in both storms. The actual quantitative values of graupel EV, hail EV, and UV10 were larger in 22 June than 29 June, but this is likely a result of the sheer size of the multicellular convection on 22 June (Figs. 4, 5, 9, 10).

The total LFR on 29 June was on the order of 100s per minute, with a maximum of 350 per minute (Fig. 10). The LFR on 22 June was also on the order of 100s per minute, though the maximum was over 500 per minute (Fig. 5), again

this is likely higher due to the larger physical size of this storm system. Regardless, both storms were extraordinarily electrically active. Both 29 June and 22 June produced mostly positive CG lightning. The 29 June supercell had positive CG flash rates of 2-4 per minute, which was similar to 22 June, except that 22 June had a peak positive CG flash rate as high as 10 per minute (Figs. 5, 10). 22 June also had more negative CG lightning than 29 June (negative CG lightning is not shown for 29 June, but was essentially negligible).

While the charge structure in 29 June was complex (as it was in 22 June), it was generally an inverted storm (Wiens et al. 2005). By the time that the 29 June supercell began producing abundant positive CGs (at 2325), the lower negative charge layer of the inverted tripole was evident. Prior to that time, the charge structure had been an inverted dipole, or a double dipole (similar to that of the early charge structure in the northern portion of 22 June). Positive CGs in both storms came to ground below the lower negative charge of an inverted tripole charge structure. The bulk of the LMA sources in 29 June were centered around 8 km, which is also the height of majority of LMA sources in 22 June (Figs. 6, 11).

5. CONCLUDING REMARKS

The objective of this study was to provide a preliminary discussion of two positive CG-producing storms. Radar and lightning observations of the 22 June 2000 storm were analyzed and compared to the observations of the 29 June 2000 supercell. The 22 June storm was a deep, multicellular storm system that produced mostly positive CG lightning and extraordinary flash rates (~500 per minute). The 29 June storm was an organized positive CG-producing supercell that also exhibited extraordinary flash rates (~300 per minute). Both storms had very complex charge structures, but inverted structures were observed in both cases, especially during times when positive CG flashes were being produced. Both storms also were kinematically intense, with maximum updrafts near 50 m s^{-1}, and large volumes of updraft greater than 10 m s^{-1}.

The volume of strong updraft has been postulated as a key factor in producing inverted storms (Lang and Rutledge 2002), whereby larger updraft volumes have limited effects from entrainment and higher supercooled liquid water contents. Laboratory work has shown that higher liquid water contents result in positive charge

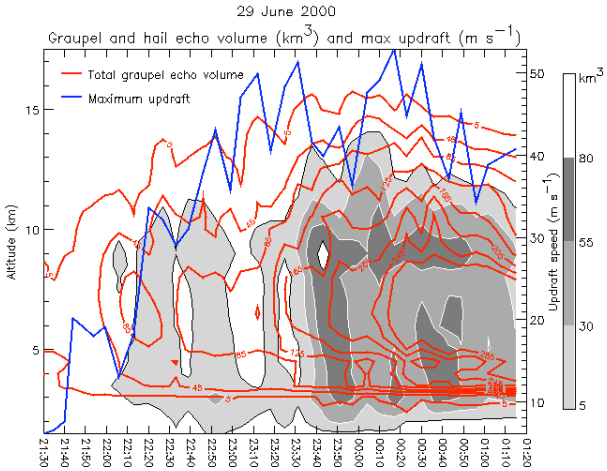

Fig. 9. Same as Fig. 4 except for 29 June 2000.

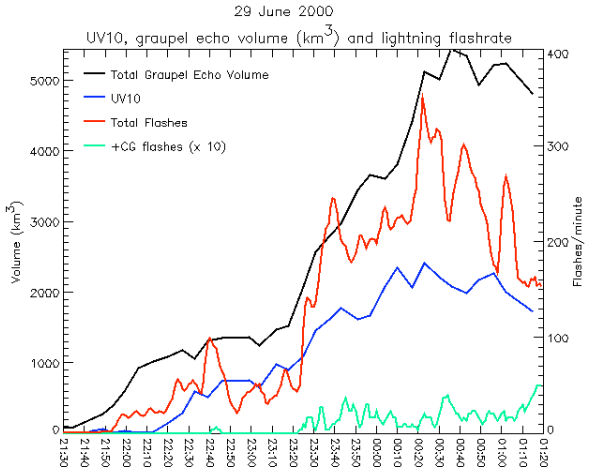

Fig. 10. Same as Fig. 5 except for 29 June 2000 and without negative CG flash rate.

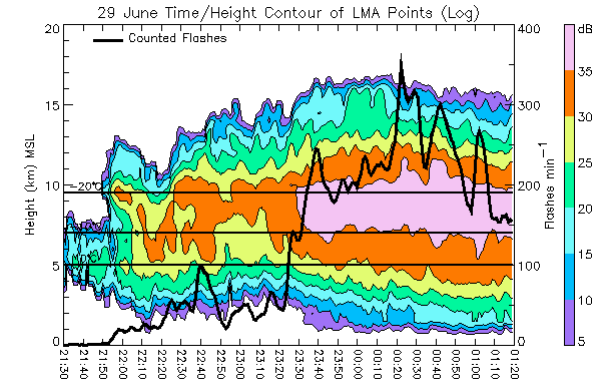

Fig. 11. Same as Fig. 6 except for 29 June 2000.

imparted to the rimer in an ice-ice collision (Takahashi 1978, Saunders et al. 1991). The volume of strong (greater than 10 m s^{-1}) updraft was indeed high in both of these storms, which is consistent with Lang and Rutledge (2002). Other common features between 22 June and 29 June are the high graupel EV and hail EV, both of which were observed throughout a great depth of the storm. Further comparative analysis and deliberation on these storms is needed before any solid conclusions can be drawn.

The LMA observations indicated that the charge structures in Cells B and C on 22 June were independently inverted even prior to the cell merger. This suggests that the local storm environment and/or microphysics may have produced the inverted structure, which is typically conducive to positive CG flashes. However, very few positive CG flashes were observed until after Cell B merged with Cell A, so it is also possible that the interaction between these two cells organized the charge layers into a configuration more favorable for positive CGs. We hope to further explore the affect of the cell merger process on lightning within this storm.

Our future work includes a detailed comparative analysis of the 29 June, 22 June, 19 June, and 3 June storms observed during STEPS. Each of these cases exhibited contrasting CG lightning activity, and we hope to gain insight on the relationships of kinematics and microphysics to the parent charge structures in each of these cases. In particular, we hope to learn more about why inverted charge structures develop, instead of the "normal" charge structure.

Acknowledgments: Support for the multiple-Doppler analysis was provided by L. Jay Miller (NCAR). Dr. Kyle Wiens (LANL) assisted us with the LMA data analysis and processing, and is to thank for use of his CDF display software. Dr. Paul Kriehbiel, Dr. William Rison, Dr. Ron Thomas, Dr. Tim Hamlin, Jeremiah Harlin, and Matt Briggs of New Mexico Tech provided the newly processed LMA data and XLMA software. We also acknowledge Drs. Rob Cifelli, Tim Lang, and Steve Nesbitt for their comments and review of this study. The CSU-CHILL radar is supported by the National Science Foundation (NSF) under grant ATM-0118021. This research was supported by the NSF Physical Meteorology Program under grant ATM-0309303.

REFERENCES

Carey, L.D., S.A. Rutledge, and W.A. Peterson, 2003: The relationship between severe storm reports and cloud-to-ground lightning polarity in the contiguous United States from 1989-98. *Mon. Wea. Rev*., **131**, 1211-1228.

Cummins, K. L., M. J. Murphy, E. A. Bardo, W. L. Hiscox, R. B. Pyle, and A. E. Pifer, 1998: A combined TOA/MDF technology upgrade of the U.S. National Lightning Detection Network. *J. Geophys. Res*., **103** (D8), 9035–9044.

Kasemir, H. W., 1960: A contribution to the electrostatic theory of lightning discharge. *J. Geophys. Res*., **65**, 1873-1878.

Lang, T.J., and S.A. Rutledge, 2002: Relationships between convective storm kinematics, precipitation, and lightning. *Mon. Wea. Rev*., **130**, 2492-2506.

Lang, T.J., and co-authors, 2004: The severe thunderstorm electrification and precipitation study. *Bull. Amer. Meteor. Soc,* in press.

Liu, H., and V. Chandrasekar, 2000: Classification of hydrometeors based on polarimetric radar measurements: Development of fuzzy logic and neuro-fuzzy systems and in situ verification. *J. Atmos. Oceanic Technol.*, **17**, 140-164.

MacGorman, D.R., W.D. Rust, P. Krehbiel, E. Bruning, and K. Wiens, 2005: The electrical structure of two supercell storms during STEPS. *Mon. Wea. Rev*., in press.

Mazur, V. and L. H. Ruhnke, 1993: Common physical processes in natural and artificially triggered lightning. *J. Geophys. Res*., **98**, 12,913-12,930.

Mohr, C.G., L.J. Miller, R.L. Vaughn, and H.W. Frank, 1986: On the merger of mesoscale data sets into a common Cartesian format for efficient and systematic analysis. *J. Atmos. Oceanic. Technol.*, **3**, 143-161.

O'Brien, J.J., 1970: Alternative solutions to the classical vertical velocity problem. *J. Appl. Meteor*., **9**, 197-203.

Rison, W., R. J. Thomas, P. R. Krehbiel, T. Hamlin, and J. Harlin, 1999: A GPS-based three-dimensional lightning mapping system: Initial observations in Central New Mexico. *Geophys. Res. Lett*., **26**, 3573-3576.

Ryzhkov, A.V. and D.S. Zrnic, 1998: Polarimetric rainfall estimation in the presence of anomalous propagation. *J. Atmos. Oceanic Technol*., **15**, 1320-1330.

Saunders, C.P.R., W.D. Keith, and R.P. Mitzeva, 1991: The effect of liquid water content on thunderstorm charging. *J. Geophys. Res.,* **96**, 11,007-11,017,.

Stolzenburg, M., W.D. Rust, and T.C. Marshall, 1998: Electrical structure in thunderstorm convective regions, 3. Synthesis. *J. Geophys. Res.,* **103**, 14,097-14,108.

Straka, J.M., D.S. Zrnic, and A.V. Ryzhkov, 2000: Bulk hydrometeor classification and quantification using polarimetric radar data: Synthesis of relations. *J. Appl. Meteor*., **39**, 1341-1372.

Takahashi, T., 1978: Riming electrification as a charge generation mechanism in thunderstorms. *J. Atmos. Sci*., **35**, 1536-1548.

Tessendorf, S.A., L.J. Miller, K.C. Wiens, and S.A. Rutledge, 2005: The 29 June 2000 supercell observed during STEPS. Part I: Kinematics and microphysics. *J. Atmos. Sci.,* in press.

Thomas, R., P. Krehbiel, W. Rison, J. Harlin, T. Hamlin, and N. Campbell, 2003: The LMA flash algorithm. Abstract C4-23, *Proc. 12th Intl. Conf. On Atmos. Elect*., 655-656, Versailles, France.

Wiens, K.C., S.A. Rutledge, and S.A Tessendorf, 2005: The 29 June 2000 supercell observed during STEPS. Part II: Lightning and charge structure. *J. Atmos. Sci.,* in press.